Power Quality Improvement of a Single-Phase Grid-Connected PV System with Fuzzy MPPT Controller

Hamad, M.S, Fahmy, A.M, and Abdel-Geliel, M.

Arab Academy for Science, Technology and Maritime Transport (AASTMT), Egypt

***Abstract*-Photovoltaic (PV) systems are grid-connected via an interfacing converter which operates with Maximum Power Point Tracking (MPPT) controller in order to feed the grid by the maximum allowable solar power. Nonlinear loads affect the system power quality. Conventionally single-phase shunt active power filter (APF) can be used to improve the power quality in terms of current harmonics mitigation and reactive power compensation. In this paper, the PV interfacing inverter is controlled using a predictive control technique to perform both functions of power quality improvement in addition to transferring the PV maximum power to the grid. A Fuzzy logic control algorithm is applied for MPPT. The proposed technique does not require an accurate system model and can easily handle system nonlinearity. The system performance is investigated using a MATLAB simulation model.**

***Index Terms*—power quality, shunt APF, predictive control, grid-connected PV systems, MPPT, Fuzzy logic control.**

I. INTRODUCTION

Harmonics is one of the power quality issues that influence to a great extent transformer overheating, rotary machine vibration, voltage quality degradation, destruction of electric power components, and malfunctioning of medical facilities [1]. Power quality improvement has been given considerable attention due to the intensive use of nonlinear loads and the limitations required by international standards such as IEEE519-1992[2].Those limitations were set to limit the disturbances and avoid major problems in power system. Since linear and/or non-linear single-phase loads are rapidly increasing, zero sequence component and current harmonics are generated. This causes overheating of the associate distribution transformers that may lead to a system failure, especially in weak networks [3]-[5].

Photovoltaic (PV) power supplied to the utility grid is gaining more and more visibility, while the world's power demand is increasing.

Global demand of electrical energy is growing by high rate due to the requirement of modern civilization. Recently, energy generated from clean, efficient and environmentally friendly sources has become one of the major challenges for engineers and scientists. Among them, PV application has received a great attention in research because it appears to be one of the most efficient and effective solutions to this environmental problem [6].

There are two topologies used to connect the PV with the grid; two stages and single stage PV system. A two stage is the traditional type and consists of a DC/DC converter direct coupled with PV array and a grid connected inverter. In single stage PV system, the DC/AC inverter has more complex control goals; Maximum Power Point Tracking (MPPT) and output current control. Regardless its control complicity, single stage PV system is more efficient and cheaper than two stages system.

For connecting the PV system to the grid, there are three widely used grid interactive PV systems; the centralized inverter system, the string inverter system and the AC module or the Module Integrated Converter (MIC) system. Among these, the MIC system offers "plug and play" concept and greatly optimizes the energy yield [7].

With these advantages, the MIC concept has become the trend for the future PV system development but challenges remain in terms of cost, reliability and stability for the grid connection [8].

Conventionally single-phase shunt active power filter (APF) uses an inverter for harmonics elimination and reactive power compensation [9]-[10].A grid connected PV system with active power filtering feature has been presented in [11]-[13].However, measuring the load current is mandatory.

In this paper, an inverter is used as a single-phase shunt active power in addition to interfacing a power of a photovoltaic (PV) as shown in Fig.1. Fuzzy Logic Control (FLC) is used as a robust controller for MPPT; this control technique can handle the model uncertainties in addition to easily handle the nonlinearity.

The single-phase shunt active power filter (APF) uses a predictive control technique to mitigate of the grid current harmonics and improve the power factor.

The proposed control strategy provides a multifunction with a simple controller incorporating Phase Locked Loop (PLL) independency, less sensors, ease of practical implementation, and reduced system size and cost. The proposed system performance is investigated for most of the conditions using a MATLAB simulation model.

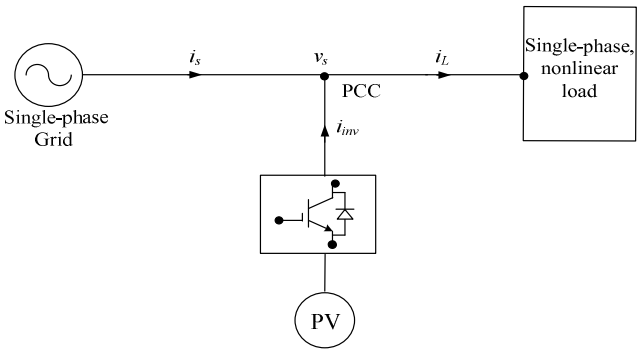

Fig. 1. Block diagram of a grid-connected PV unit

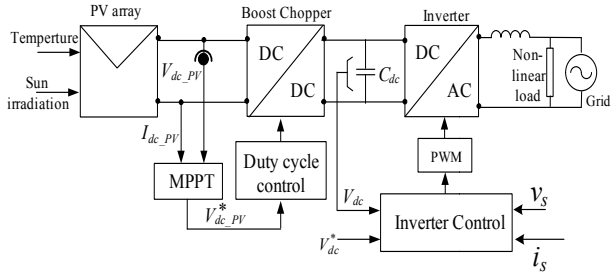

Fig. 2. The Overall system modelling including control signals

II. PV SYSTEM MODELING

The single-phase multi stage grid connected system is shown in Fig. 2. It consists of a PV array followed by step up stage, which feeds a predictive current controlled voltage source inverter acts as an APF that feeds current into the single phase grid and linear/non-linear single phase loads.

A. Photovoltaic Cell equivalent circuit

The traditional equivalent circuit of a solar cell is represented by a current source in parallel with one or two diodes. A single-diode PV cell model form is illustrated in Fig. 3, including four components: a photo current source, I_{ph}, a diode parallel to the source, a series resistor, R_s, a shunt resistor, R_{sh}. The DC current generated, I_{ph}, when the cell is exposed to light varies linearly with solar irradiance [14]. The shunt resistance R_{Sh} is inversely related with shunt leakage current to the ground. In general, the PV efficiency is insensitive to variation in R_{Sh} and the shunt-leakage resistance can be assumed to approach infinity without leakage current to ground. The net cell current of the cell is the difference of the light-generated current, I_{ph}, and the diode current, I_d, as shown in Fig. 4. Equation (1) describes the I-V characteristic of the ideal photovoltaic cell.

$$I = I_{PV,CELL} - I_{O,CELL}\left[\exp\left(\frac{qV}{akT}\right) - 1\right] \quad (1)$$

where $I_{pv,cell}$ is the current generated by the incident light (it is directly proportional to the sun irradiation), $I_{0,cell}$ is the leakage current, q is the electron charge [1.60217646×10^{-19}C], k is the Boltzmann constant [1.3806503×10^{-23} J/K], T is the temperature of the p-n junction, and a is the diode ideality constant.

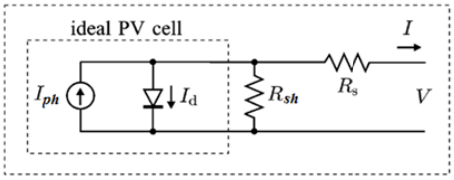

Fig.3 Single-diode model of theoretical PV cell [5]

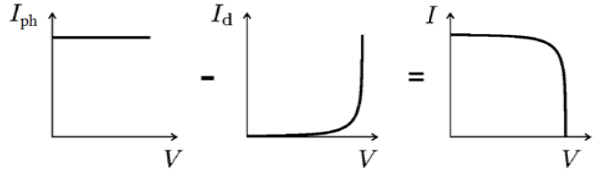

Fig. 4 PV cell I–V curves [5].

Practical arrays are composed of several connected photovoltaic cells and the observation of the characteristicsat the terminals of the photovoltaic array requires the inclusion of additional parameters to the basic equation (2):

$$I = I_{PV} - I_O\left[\exp\left(\frac{V+R_s}{V_t a}\right) - 1\right] - \frac{V+R_S I}{R_P} \quad (2)$$

where I_{pv} and I_0 are the photovoltaic and saturation currents of the array and $V_t = (N_s kT)/q$ is the thermal voltage of the array with N_s cells connected in series.

The light generated current of the photovoltaic cell depends linearly on the solar irradiation and is also influenced by the temperature according to (3) [15]:

$$I_{PV} = (I_{PV,n} + K_I \Delta T)\frac{G}{G_n} \quad (3)$$

where $I_{pv,n}$ is the light-generated current at the nominal condition (usually 25˚C and 1000W/m^2),$\Delta T = T - T_n$ (being T and T_n the actual and nominal temperatures), G [W/m^2] is the irradiation on the device surface, and G_n is the nominal irradiation. The diode saturation current I_0 and its dependence on the temperature may be expressed by equation (4) [16]:

$$I_O = (I_{O,n}(\frac{T_n}{T})^3 \exp\left[\frac{qE_g}{ak}(\frac{1}{T_n} - \frac{1}{T})\right] \quad (4)$$

*w*here E_g is the band gap energy of the semiconductor ($E_g \approx$ 1.12 eV for the polycrystalline Si at 25˚C [17]), and$I_{0,n}$is the nominal saturation current.

III. MODEL OF FLY-BACK DC-DC CONVERTER

For grid-connected PV applications, two topologies of the PV energy conversion systems have been mostly presented; known as one-stage and two stage systems. This paper focuses on the two-stage PV energy conversion system, because it offers an additional degree of freedom in the operation of the system when compared with the one-stage configuration, in addition to decreasing the global efficiency of the combined system because of the connection of two cascade stages. Therefore, by including a DC-DC converter between the PV array and the inverter connected to the electric grid, various control objectives are possible to track concurrently with the PV system operation.

The converter is linked to the PV system with a filter capacitor C to reduce the high frequency ripples due to transistor switching. The DC-DC converter output is connected to the DC bus of the DC-AC converter, as depicted in Fig.5, and produces a chopped output voltage, therefore controls the average DC voltage relation between its input and output. So the PV system and the DC-AC converter are matching. The steady-state voltage and current relations of the boost converter operating in continuous current mode are [18]:

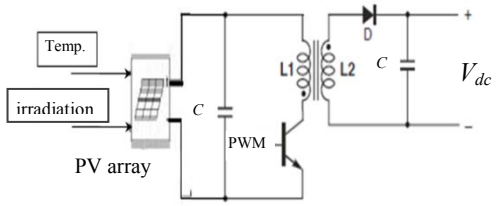

Fig. 5 Grid-connected PV system with boost DC-DC converter.

$$V_D = \frac{V_{PV}}{1-D} \quad (5)$$

$$I_D = \eta_b(1-D)I_{PV} \quad (6)$$

where:

η_b: Efficiency of the boost converter

D: DC-DC converter duty cycle

I_{pv}: PV array output current

V_{pv}: PV array output voltage

I_D: DC bus current (inverter side)

V_D: DC bus voltage (inverter side)

The fly-back transformer provides isolation and also the voltage ratios are multiplied by turn's ratio. Fly-back transformer model includes an inductance Lm and an ideal transformer with a turn's ratio N_1/ N_2. The leakage inductance and losses of the Fly-back transformer are neglected here. But the leakage inductance affects the switch and diode transitions.

$$V_0 = ABS(V_g)\left(\frac{\mathrm{D}}{(1-\mathrm{D})}\right)\left(\frac{N_2}{N_1}\right) \quad (7)$$

$$I_g = I_0\left(\frac{\mathrm{D}}{(1-\mathrm{D})}\right)\left(\frac{N_2}{N_1}\right) \quad (8)$$

The magnitude of L_m decides the boundary between Continuous and Discontinuous Current Modes(CCM and DCM). The series connection of switch S_1 with DC generator results in pulsating input current [19].

IV. Proposed MPPT Using Fuzzy Logic Control

In order to track the time varying maximum power point of the solar array depending on its operating conditions of insulation and temperature, the MPPT control technique plays an important role in the practical PV systems. A variety of MPPT schemes and several sensor-less approacheshave been proposed in the literatures [20].

This paper proposes MPPT control technique with FLC. The output power of PV arrays varies with weather conditions; solar irradiation and atmospheric temperature. Therefore, real time MPPT control for extracting maximum power from the PV panel becomes indispensable in PV generation systems [21]-[22].

MPPT using FLC gains several advantages of better performance, robust and simple design. In addition, this technique does not require the knowledge of the exact model of the system and it can handle the nonlinearity. The main parts of FLC; fuzzification, rule-base, inference and defuzzification, are shown in Fig.6.

MPPT using FLC provides better performance, robust and simple design. The proposed FL-MPPT Controller is shown in Figure 7.It has two inputs and one output. The two FLC input variables are the error E and change of error CE at sampled times j defined by

$$P_{PV} = V_{PV} * I_{PV} \quad (9)$$

$$E(j) = \frac{P_{PV}(j)-P_{PV}(j-1)}{V_{PV}(j)-V_{PV}(j-1)} \quad (10)$$

$$CE(j) = E(j) - E(j-1) \quad (11)$$

where P_{pv}, I_{PV}, V_{pv} are the PV power, current and voltage respectively at instant j.

E (j) shows that if the load operating point at the instant j is located on the left or on the right of the maximum power point on the P-V characteristic where it is equals to zero at MPP. While the change of error $CE(j)$ expresses the moving direction of this point where the control action duty cycle D used for the tracking of the MPP by comparing with the saw tooth waveform to generate a PWM signal for the fly-back boost converter [23].

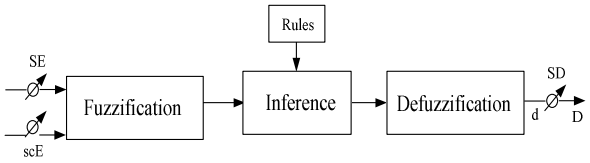

Fig.6 Fuzzy controller diagram

For example, if the operating point is far to the left of the MPP, that is E is PB, and CE is ZE, then it is required to largely increase the duty ratio i.e., D should be PB to reach the MPP. In the defuzzification stage, the fuzzy logic controller output is converted from a linguistic variable to a numerical variable still using a membership function. This provides an analog signal that will control the power converter to the MPP [24].

In this paper Mamdani's fuzzy inference method, with Max-Min operation fuzzy combination has been used.

The membership functions for the variable are shown in Fig. 7.The control rules are indicated in table 1with E and CE as inputs and D as the output.

Table 1: Fuzzy rules base

E / CE	NB	NS	ZE	PS	PB
NB	ZE	ZE	PB	PB	PB
NS	ZE	ZE	PS	PS	PS
ZE	PS	ZE	ZE	ZE	NS
PS	NS	NS	NS	ZE	ZE
PB	NB	NB	NB	ZE	ZE

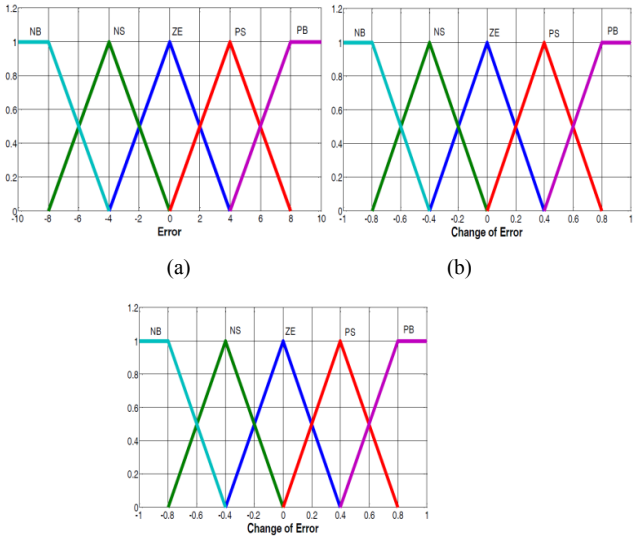

Fig.7. Membership function of (a) error E - (b) change of error CE - (c) duty ratio D

V. PROPOSED INVERTER CONTROL TECHNIQUE

The proposed system shown in Fig. 8 consists of PV array, Boost chopper, DC-link capacitor, and a multifunctional inverter connected at the PCC to a single-phase grid through the interface inductances. The compensator reference current is calculated from the sensed grid current drawn by nonlinear and single-phase loads connected to the grid. The reference current is computed by using capacitor voltage control [25]. The compensation objective is to compensate for load current harmonics, reactive power compensation and to regulate the DC bus during bidirectional active power exchange between the DC side load/source and the power system grid.

The compensation functions are executed simultaneously where a single-phase nonlinear load are fed from both the gird and the PV system. The performance is tested for the following cases:

Case 1: at normal condition.

Case 2: the load increases.

Case 3: the solar irradiation decreases.

Case 4: the atmospheric temperature increases.

The proposed control system block diagram is shown in Fig. 8. The multifunctional inverter is controlled with a predictive control strategy. It requires the measurement of the grid voltage and current at PCC and the inverter DC-link voltage. The measurement of the load current and the injected inverter current are not required. The inverter reference current is extracted using DC-link capacitor voltage control method. The DC-link voltage, V_{dc}, are subtracted from the reference voltage, V^*_{dc}. A *PI*-controller acts on the resultant error. The DC-link voltage is maintained constant and the power balance between the grid, inverter, and the load is achieved as the capacitors compensate instantaneously the difference between the grid and the load power [26]-[29].

The multiplication of the *PI*-controller output with the PCC per unit voltage forms the grid current reference. Ideal grid voltage is assumed. The reference and measured grid currents and the PCC voltage are used to predict the inverter reference voltage required to force the actual current to track its reference.

The predictive current control presented in [27] is used to control the interfacing power converter of the DG unit. The predicted converter output voltage is expressed in terms of the reference and actual grid currents by

$$v_c^*(k+1) = L_i\left(\frac{i_s(k) - i_s^*(k)}{T_s}\right) + v_s(k) \tag{12}$$

where, L_i is the interfacing inductance, T_s is the sampling time. $i_s^*(k)$ and $i_s(k)$ are the sinusoidal reference and the measured grid current at sampling instant k, respectively. v_s is the grid voltage.

The grid reference current $i_s(k)$ in (13) represents single-phase sinusoidal grid current. The introduced sampling time delay is less significant sampling frequency is high [28].

Therefore, the predictive control method proposed for the multifunctional inverter can compensate both of the grid current harmonics and reactive power required also transfers the PV power, thus grid current become sinusoidal and the DC bus are regulated during bidirectional active power exchange between the DC side load/source and the grid. This method provides simple control algorithm without a PLL, minimizes the number of sensors as the load and inverter currents are not measured, and provides ease of practical implementation.

VI. PERFORMANCE INVESTIGATION OF THE PROPOSED SYSTEM

The proposed system shown in Fig. 2 is simulated using a MATLAB/Simulink model to investigate its performance.The system parameters are listed in table 2 and the high frequency transformer parameters of the fly-back DC-DC converter shown in Fig. 5, are listed in table 3.

The PCC voltage is 220 V. The non-linear load is represented by a single-phase diode rectifier feeding an inductive load representing a harmonic current producing source. The resistance and the inductance of the inverter coupling inductor, are R_i = 0.05 Ω and L_i = 3.2 mH respectively. DC-link capacitor of 3.0 mF is used. The reference voltage for this loop is set at 420V and the inverter switching frequency, f_s, is 5 kHz.

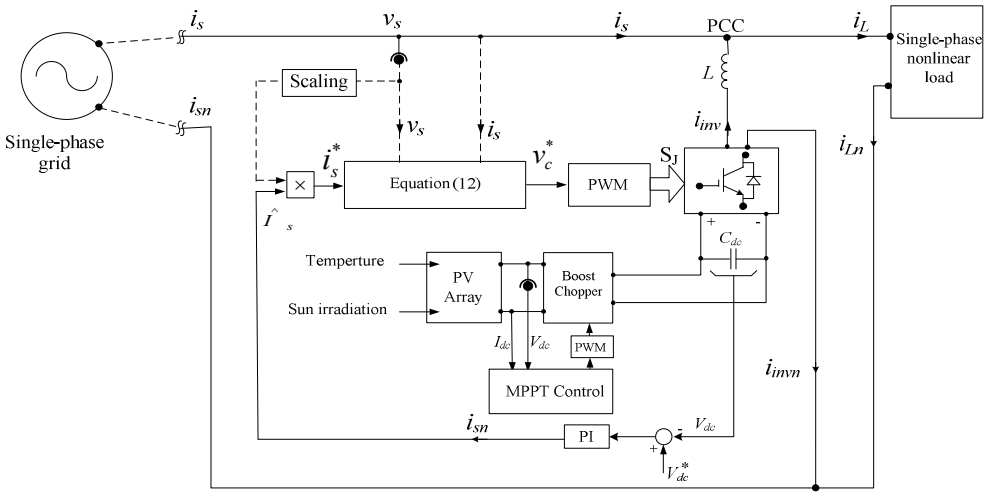

Fig. 8. Block diagram of the proposed control of inverter

Table 2: The system parameters

Symbol	Quantity	Values
P_{MPPT}	Rated power	199 W
V_{MPPT}	Rated voltage	26.3 V
I_{MPPT}	Rated current	7.6 A
V_{OC}	Open-circuit voltage	32.9 V
I_{SC}	Short-circuit current	8.21 A
N_S	Number of series cell	54
N_P	Number of parallel cell	1
N_{Sm}	Number of series module	1
N_{Pm}	Number of parallel module	1
C	PV module capacitor	4700µF
T_C	Atmospheric Temperature	25°C
G_N	Solar Irradiation	1000 W/m^2
V_S	Grid voltage in RMS	220 V
V^*_{dc}	DC reference voltage	420V
C_F	Fly-back capacitor	3.0mF
L_S	Grid tied inductor	3.2mH
C_{dc}	DC-bus capacitor	5 µF
F_{SM}	Sampling frequency	33kHz
F_{SW}	Switching frequency	5kHz
F	Line frequency	50Hz

Table 3: Fly-back HF transformer parameters

Quantity	Symbol	Values
Inductance	L_{boost}	28µH
DC resistance	DCR Primary	0.008 Ohms
DC resistance	DCR Secondary	0.472 Ohms
Self-Resonant Frequency	SRF	360 kHz
Saturation current	I_{sat}.	10.5 A
Turns ratio	Pri: Sec	1:12

The system performance is investigated for the following cases:

Case 1: from 0.2 to 0.4 s; a single-phase nonlinear load of 250 W is fed from both the gird and the PV unit at solar irradiation of 1000 W/m^2 and an atmospheric temperature of 25°C.

Case 2: at 0.4 s, the load increases to 400 W.

Case 3: at 0.6 s, the solar irradiation decreases to 900 W/m^2.

Case 4: at 0.8 sec, the temperature increases to 35°C.

The simulation results are shown in Fig. 9. The grid voltage waveforms at the PCC, v_s, are shown in Fig. 9(a). Typical non-linear load current, i_L, is shown in Fig. 9(b). Its total harmonic distortion (THD) is 31 %. The inverter current, i_{inv}, injected at the PCC is shown in Fig. 9(c). As a result, sinusoidal grid current, i_s, with near unity power factor is achieved as shown in Fig. 9(d). The grid current THD is compared before and after compensation. The APF improves the THD from 31% to 3.2% which comply with the IEEE Std. 519-1992. An almost steady DC-link voltage, V_{dc} , is shown in Fig. 10. The load active and reactive power P_L, Q_L are increased from 250 W to 400 W and from 50 VAR to 80 VAR as shown Fig. 11(a). The active and reactive power of the grid are shown in Fig. (b), the grid active power, P_s are increased from 130 W to 250 W while the grid reactive power Q_s maintained near zero. Fig.11(c) presents the power supplied by the PV unit which is almost maintained at 140 W with small variations duo to the change of solar irradiation and atmospheric temperature.

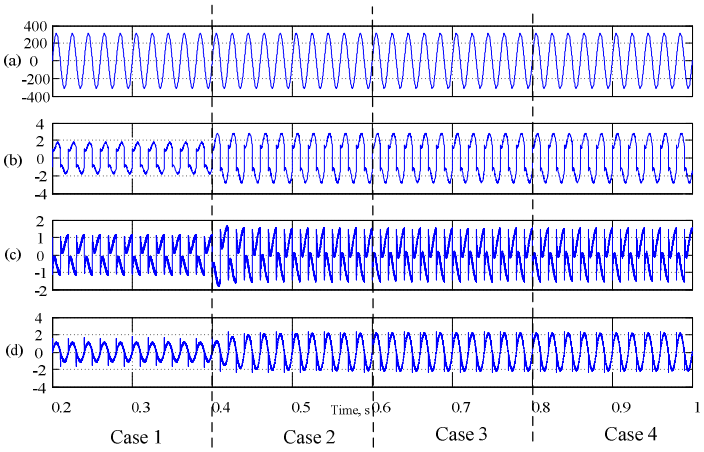

Fig.9. Simulation results: (a) grid voltage, v_s(V), (b) load current, i_L(A), (c) inverter current, i_{inv}(A), and (d) grid current, i_s(A).

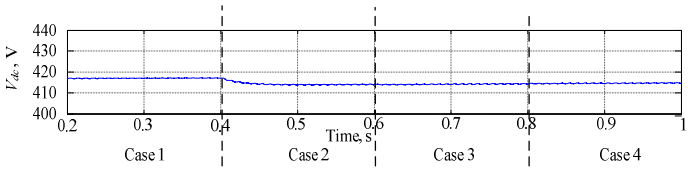

Fig. 10. Simulation results: the capacitor voltage, V_{dc}

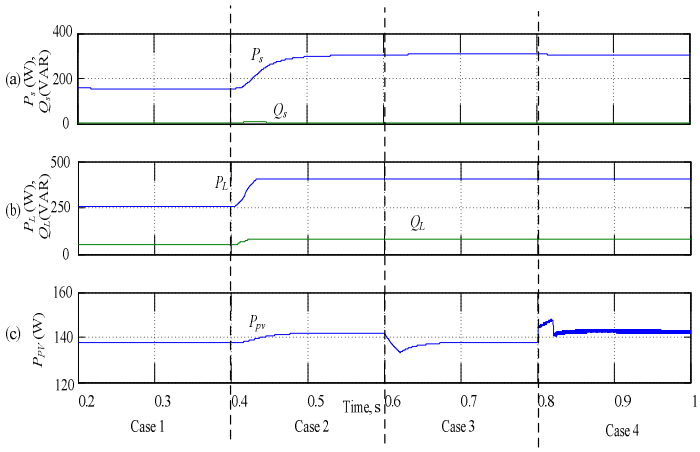

Fig. 11. Simulation results: (a) grid active and reactive power, P_s and Q_s, (b) load active and reactive power, P_L and, Q_L and(c) PV supplied Power P_{PV}

VII. CONCLUSION

In this paper, a PV system is interfaced to the grid via a multifunctional interfacing inverter. A MPPT fuzzy logic controller is employed to feed the grid by the maximum allowable PV power. A simple predictive current control algorithm is used. The system performance is investigated using a MATLAB/ Simulink model at different cases of load variation, atmospheric temperature variation and solar irradiation variation. The inverter achieves functions of supplying the available power from the PV unit into the loads in addition to improving the power quality in terms of grid current THD and power factor. The results comply with the limits of the IEEE Std. 519-1992.

REFERENCES

[1] R.D. Henderson, and P. J. Rose, "Harmonics: The effects on power quality and transformers," IEEE Transaction on Industrial Applications, Vol.30, No.3, May/Jun 1994, pp.528-532.

[2] IEEE Std. 519-1992, Recommended Practices and Requirements for Harmonic Control in Electric Power Systems, 1992.

[3] T.M. Gruzs, "A survey of neutral currents in three-phase computer power systems, Industry Applications, ," IEEE Transaction on Industrial Electronics, Vol.26, No.4, Jul/Aug 1990, pp.719-725.

[4] F. Liu, X. Zhang, Z. Xie, P. Xu, and L. Chang, "Shunt active power filter for harmonic and reactive current compensation in wind conversion systems," IEEE Power Electronics Specialists Conference, PESC, 2008, pp.2329-2332.

[5] B. Singh, and S. Sharma, "SRF theory for voltage and frequency control of IAG based wind power generation," IEEE International Conference on Power Systems, ICPS 2009, pp.1-6

[6] T. Shimizu, O. Hashimoto, and G. Kimura, "A novel high performance utility-interactive photovoltaic inverter system." IEEE Transaction on Power Electronics, Vol. 18, No. 2, Feb. 2003, pp. 704–711.

[7] S. B. Kjær, J. K. Pedersen, and F. Blaabjerg, "A review of single-phase grid-connected inverters for photovoltaic modules," IEEE Transaction on Industrial Applications, Vol. 41, No. 5, Sep./Oct. 2005, pp. 1292–1306.

[8] J. M. Carrasco, *et.al.*, "power-electronic systems for the grid integration of renewable energy sources: A survey," IEEE Transaction on Industrial Electronics, Vol. 53, No. 4, Aug. 2006, pp. 1002–1016.

[9] S.G. Pinto,*et. al.*, "Single Phase Active Filter with digital control, International Conference on Renewable Energies and Power Quality, ICREQ´07, March 2007, pp. 28-30.

[10] P. Neves, ,*et. al.*, "Experimental Results of a Single- Phase Shunt Active Power Filter Prototype with different switch techniques," IEEE International Symposium on Industrial Electronics Vigo, 2007.

[11] L. Cheng, R. Cheung, K. H. Leung, "Advanced photovoltaic inverter with additional active power line conditioning capability," IEEE Power Electronics Specialists Conference,1997, pp. 279–283.

[12] S. Kim, G. Yoo, and J. Song, "A Bi-functional utility connected photovoltaic system with power factor correction and facility", Proc. Photovoltaic Specialists Conference,1996, pp. 1363–1368.

[13] T. Wu, C. Shen, H. Nein, and G. Li, "A 1φ/3W inverter with grid connection and active power filtering based on nonlinear programming and fast-zero-phase detection algorithm", IEEE Transactions on Power Electronics, Vol.20, No.1, Jan.2005, pp. 218 – 226.

[14] M.G. Villalva, J.R. Gazoli, and E.R. Filho, "Comprehensive Approach to Modeling and Simulation of Photovoltaic Arrays, "IEEE Transactions on Power Electronics, Vol. 24, No.5, May 2009, pp.1198-1208.

[15] D. Sera, R. Teodorescu, and P. Rodriguez, "PV panel model based on datasheet values," Proceeding of IEEE International Symposium on Industrial Electronics, ISIE 2007, pp. 2392–2396.

[16] J. Crispim, M. Carreira, and R. Castro, "Validation of photovoltaic electrical models against manufacturers data and experimental results," International Conference on Power Engineering, Energy and Electrical Drives, POWERENG, 2007, pp. 556–561.

[17] M.G. Molina, and P.E. Mercado, "Modeling and Control of Grid-connected PV Energy Conversion System used as a Dispersed Generator," IEEE Transmission and Distribution Conference and Exposition, 2008, pp. 1 – 8.

[18] E. Duran, J. Cardona, M. Galan, and J.M. Andjar, "Comparative Analysis of Buck-Boost Converters used to obtain I-V characteristic curves of Photovoltaic Modules," IEEE Power Electronics Specialists Conference, 2008, pp. 2036 – 2042..

[19] H. Sugimoto, *et. al.*, "A new scheme for maximum photovoltaic power tracking control," IEEE Power Conversion Conference, Nagaoka 1997, Vol.2, pp.691-696.

[20] M. Matsui, *et. al.*, "New MPPT Control Scheme Utilizing Power Balance at DC Link Instead of Array Power Detection," IEEE 27th Annual Conference on Industrial Electronics Society, IECON 2001. Vol.1, pp. 164-169.

[21] T. Esram and P.L. Chapman, "Comparison of Photovoltaic Array Maximum Power Point Tracking Techniques," IEEE Transaction on Energy Conversion, Vol.22, No.2, June 2007, pp.439-449.

[22] G.M.S. Azevedo, M.C. Cavalcanti, and K.C. Oliveira, "Evaluation of Maximum Power Point Tracking Methods for Grid Connected Photovoltaic Systems," IEEE Power Electronics Specialists Conference, June, 2008, pp. 1456-1462.

[23] A. Panda, M.K. Pathak, and S.P. Srivastava, "Fuzzy Intelligent Controller for The Maximum Power Point Tracking of a Photovoltaic Module at Varying Atmospheric Conditions", Journal of Energy Technologies and Policy, Vol.1, No.2, 2011, pp.18-27.

[24] T. Senjyu and K. Uezato, "Maximum power point tracker using fuzzy control for photovoltaic arrays," IEEE International Conference of Industrial Technology, 1994, pp. 143–147.

[25] S. Huang and J.C. Wu, "A control algorithm for three-phase three-wired active power filters under non-ideal mains voltages," IEEE Transaction on Industrial Electronics, Vol. 14, Jul 1999, pp. 153-760

[26] G. Brando, A. Del Pizw, and E. Faccenda. "A Comparison Between Some Control Algorithms of Parallel Active Filtering," 4th Annual IEEE Conference on Devices, Circuits and Systems, April 2002, pp. 14-20.

[27] A. Fahmy, M.S. Hamad, A.K. Abdelsalam, and A. Lotfy, "Power quality improvement in three-phase four-wire system using a shunt APF with predictive current control," IEEE 38th Annual Conference on Industrial Electronics Society, IECON, 25-28 Oct. 2012, pp.668-673.

[28] S. Jeang and M.H Wu, "DSP-based Active Power Filter with Predictive Current Control," IEEE Transaction on Industrial Electronics, Vol. 44, No. 3, Jun 1997, pp. 329-336.